International Journal of Mechanical, Industrial and Aerospace Sciences
ISSN: 2517-9950
Vol:9, No:2, 2015

Flutter Analysis of Slender Beams with Variable Cross Sections Based on Integral Equation Formulation

Z. El Felsoufi, L. Azrar

***Abstract*—**This paper studies a mathematical model based on the integral equations for dynamic analyzes numerical investigations of a non-uniform or multi-material composite beam. The beam is subjected to a sub-tangential follower force and elastic foundation. The boundary conditions are represented by generalized parameterized fixations by the linear and rotary springs. A mathematical formula based on Euler-Bernoulli beam theory is presented for beams with variable cross-sections. The non-uniform section introduces non-uniformity in the rigidity and inertia of beams and consequently, more complicated equilibrium who governs the equation. Using the boundary element method and radial basis functions, the equation of motion is reduced to an algebro-differential system related to internal and boundary unknowns. A generalized formula for the deflection, the slope, the moment and the shear force are presented. The free vibration of non-uniform loaded beams is formulated in a compact matrix form and all needed matrices are explicitly given. The dynamic stability analysis of slender beam is illustrated numerically based on the coalescence criterion. A realistic case related to an industrial chimney is investigated.

***Keywords*—**Chimney, BEM and integral equation formulation, non uniform cross section, vibration and Flutter.

I. Introduction

THE interest in non-uniform beam due to cross variable section or to non uniformity material has been widespread in recent year due to the structural advantage of such form in some system. The free vibration problem has been studied by a lot of researchers. However, for a non uniform beam, even without any other parameters, the researches on their dynamic behaviors are relatively fewer [1], [2]. For designers and manufacturing systems, the rectangular and the circular cross sections are usually used. As to the free vibration and the dynamic analyses of those non uniform beams carrying multiple parameters (concentrated foundations or masses, fixations, etc.), the information concerned is rare and this is one of the reasons why the problem in this aspect is studied. Literature relating to the free vibration analysis of a non-uniform beam is rare [3]. The numerical assembly method presented in [4], takes the case with any number of concentrated attachments. Instability phenomenon of non–uniform beam is inexistent. Amongst the numerical methods available for thin structure problems, the finite element method is undoubtedly the most versatile. The only problem with this method is that its formula is quite laborious and it takes a large amount of computer storage. A powerful alternative method based on integral equations is the Boundary Element Method (BEM) [5], [6]. The main reason for rapid development of the BEM is a dimensionality reduction possibility of the problem, leading to a reduced set of equations and a smaller amount of data required to calculate. For a part of problem, is using the fundamental solution corresponding to the exact solution, inappropriate terms are moved to the right hand side of governing equation and considered as a fictitious source density. For dynamic instability of a non uniform beams under elastic foundations and sub-tangential follower forces, domain integrals are necessary in formulation. Thus, the main advantage of dimensionality reduction is eliminated. But, the use of Dual Reciprocity Method (DRM), introduced by Nardini and Brebbia [7], permits to combine the dimensionality reduction advantage with a simple fundamental solution and to formulate the problem on boundary unknowns only. A comprehensive literature review of the DRM and Multiple Reciprocity Method (MRM) as applied to elasto-dynamics can be found in [8]. Karimi Khorramadi and A.R. Nezamabadi [9] give a studies free vibration of functionally graded beams subjected to axial load that is simply supported at both ends lies on a continuous elastic foundation. Displacement field of beam is assumed based on Engesser-Timoshenko beam theory. The Young's modulus of beam is assumed to be graded continuously across the beam thickness

In this paper, we present a general formula based on integral equation formulation for the investigation of dynamic analysis (buckling, vibration, dynamic instability, …) of a non uniform slender beam with a generalized fixations submitted to an elastic foundation and to a follower force.

II. Basic Beam Equations

Based on the Euler-Bernoulli theory for slender beams and neglecting the axial displacement, the equation of motion is formulated using the transverse displacement only. The fixations are generalized by the introduction of linear and rotary springs at the two ends of the beams as presented in Fig. 1. The partial differential equation governing the motion of beams subjected to sub-tangential force, lateral excitation and boundary generalized fixations is formulated by:

$$\frac{\partial^2}{\partial z^2}\left[EI(z)\ \frac{\partial^2 V(z,t)}{\partial z^2}\right]+\rho S(z)\left(\frac{\partial^2 V(z,t)}{\partial t^2}\right)+\ \kappa(z)\ V(z,t)+\ \lambda(z)\frac{\partial^2 V(z,t)}{\partial z^2}=p(z,t) \tag{1}$$

Z. Elfelsoufi is with the Equipe de Modélisation Mathématique et Contrôle, UFR SPI. Faculté des Sciences et Techniques de Tanger, Université Abdelmalek Essaädi, BP. 416; Tanger, Maroc (corresponding author, phone: (00 212) 661 71 72 56; fax: (00 212) 539 39 39 53; e-mail: elfelsoufi_zoubir@yahoo.fr).

L. Azrar is with the Equipe de Modélisation Mathématique et Contrôle, UFR SPI. Faculté des Sciences et Techniques de Tanger, Université Abdelmalek Essaädi, BP. 416; Tanger, Maroc (e-mail: azrarlahcen@yahoo.fr).

where V is the transverse displacement, E, I, S and ρ are the Young's modulus, the inertia, the area and the mass density respectively. λ is the sub-tangential load, κ is the elastic foundation, *p(z,t)* is the lateral excitation and z is the axial coordinate. The boundary fixations will be discussed later. For a slender beam with a non uniform cross section, the section *S(z)* and the inertia *I(z)* are *z*-abscissa dependent. Splitting the inertia and the section into constant and variable parts, the following equations may be used:

$$E\,I(z) = E\,I(0)\left(1 + K1(z)\right) \text{and } \rho\,S(z) = \rho\,S(0)\,K2(z) \qquad (2)$$

where *S(0)* and *I(0)* are the section and the inertia at the end (*z=0*). *K1(z)* and *K2(z)* depend on the type of section considered and translate the inertia and section variation along the beam. Remember that the function *K1(z)* depends also on the sense of displacement considered and particularly when the section is rectangular.

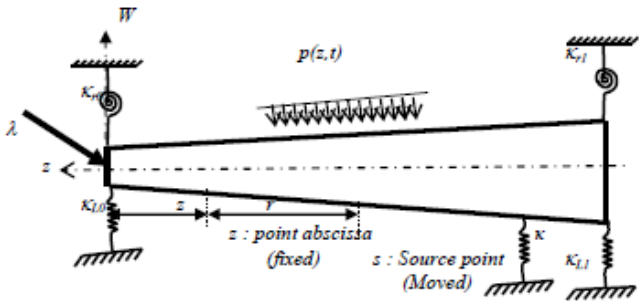

Fig. 1 A non uniform beam with circular section, linear variation and generalized fixations

Equation (1) is a partial differential equation with variable coefficients. The principal part of this equation is the rigidity term $\frac{\partial^2}{\partial z^2}\left(EI(z)\ \frac{\partial^2 V(z,t)}{\partial z^2}\right)$ which can be decomposed using (2) as:

$$\frac{\partial^2}{\partial z^2}\left(EI(z)\ \frac{\partial^2 V(z,t)}{\partial z^2}\right)$$
$$= EI(0)\frac{\partial^4 V(z,t)}{\partial z^4} + EI(0)\frac{\partial^2}{\partial z^2}\left(K1(z)\ \frac{\partial^2 V(z,t)}{\partial z^2}\right) \qquad (3)$$

Then, we obtain the following adimentional equation:

$$\frac{\partial^4 W}{\partial x^4} + \frac{\partial^2}{\partial x^2}\left[K1(x)\ \frac{\partial^2 W}{\partial x^2}\right] + K2(x)\,\ddot{W} + \kappa^*(x)\,W + \lambda^*\frac{\partial^2 W}{\partial x^2} = p^* \qquad (4)$$

where

$$\chi^2 = \frac{\rho S(0) L^4}{EI(0)},\ \kappa^* = \kappa\frac{L^4}{EI(0)},\ \lambda^* = \lambda\frac{L^2}{EI(0)},\ p^* = p\frac{L^3}{EI(0)},$$
$$W(x,\tau) = \frac{V(z,t)}{R},\quad \tau = \frac{t}{\chi},\quad R = \sqrt{\frac{I}{S}} \text{ and } x = \frac{z}{L}.$$

R is the radius of gyration of the beam, $0 \le x \le 1$ and $\dot{(\,)}$ indicates time derivative.

The aim of this paper is the development of integral equation formulations for numerical solutions of (4) with generalized boundary conditions and dynamical behaviors of non-uniform slender beams subjected to various types of loads.

A. Cross Section Considered

In manufacturing engineering beam systems, the case of a constant cross section is very limited and variable cross section offers various performances that are very useful. Most cross sections used in manufacturing beam systems are circular or rectangular. Non uniformity of the section introduces a non uniformity in rigidity and inertia of beams that leads to intricate governing equilibrium equation. In this study, we limit ourselves to beams with circular cross sections and constant young modulus and mass density. This type of section is simply characterized by its radius or diameter. The sense of transverse displacement has no effect in this type of section. For a parabolic variation (Fig. 2), diameter and inertia of section are given by:

$$d(x) = d_0\left(r_1 x^2 + r_2 x + 1\right).$$
$$d(0) = d_0,\quad d(0.5) = d_2 \quad \text{and} \quad d(1) = d_1 \qquad (5)$$

$$I(x) = I_0\left[1 - K1(x)\right] \qquad (6)$$

where

$$K1(x) = \left(r_1 x^2 + r_2 x + 1\right)^4 - 1\ ;\ K2(x) = \left(r_1 x^2 + r_2 x + 1\right)^2;$$
$$r_1 = 2\frac{d_1}{d_0} - 4\frac{d_2}{d_0} + 2 \text{ and } r_2 = 4\frac{d_2}{d_0} - \frac{d_1}{d_0} - 3 \qquad (7)$$

In case of a convex $(d_0 = d_1\,;\, d_0 < d_2)$ or a concave $(d_0 = d_1\,;\, d_0 > d_2)$ section, we have:

$$r = r_1 = -r_2 = 4\left(1 - \frac{d_2}{d_0}\right)$$

Inertia and mass functions are reduced to:

$$K1(x) = \left(r\,x^2 - r\,x + 1\right)^4 - 1 \text{ and } K2(x) = \left(r\,x^2 - r\,x + 1\right)^2 \qquad (8)$$

An emphasis is on a particular section corresponding to a circular one with linear variation (Figs. 3 (a) and (b)) obtained for $d_2 = \frac{1}{2}(d_1 + d_0)$. For this type of section, $r_1 = 0$ and $r_2 = \frac{d_1}{d_0} - 1$. Inertia and section functions are then given by:

$$K1(x) = \left((r-1)x + 1\right)^4 - 1 \text{ and } K2(x) = \left((r-1)x + 1\right)^2,\ r = \frac{d_1}{d_0} \qquad (9)$$

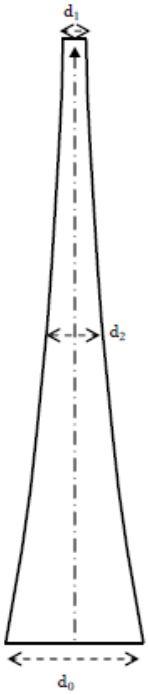

Fig. 2 A non uniform beam with circular section and parabolic variation

Fig. 3 (a) A geometrical model of a beam with large basis (r < 1)

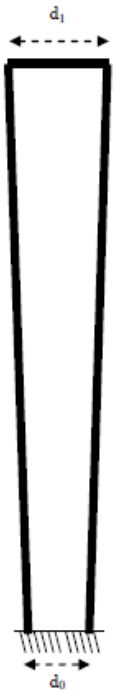

Fig. 3 (b) A geometrical model of a beam with reduced basis ($r > 1$)

B. Integral Equation Formulation

Equation (4) can be directly treated by Integral Equation Formulation when fundamental solution of the operator $\frac{\partial^2}{\partial x^2}\left(K1(x)\ \frac{\partial^2}{\partial x^2}\right)$ is analytically known. Unfortunately, this fundamental solution is known only for a few cases of simplified functions $K1(x)$. In this study, only fundamental solution of the simplified operator will be used. Let us denote W^* fundamental solution of the following problem:

$$\frac{\partial^4 W^*(x,s)}{\partial x^4} = \delta(x,s) \tag{10}$$

where δ is Dirac function and s is the source point. This fundamental solution will be used and the partial differential equation (4) will be transformed into an integral equation. Following the boundary element procedure [5], [6], resulting integral equation will be reduced to an algebro-differential equation that will be solved by the dual reciprocity method. Multiplying (4) by W^* and integrating from 0 to 1, we obtain:

$$\int_0^1 \frac{\partial^4 W(x)}{\partial x^4} W^*(x,s)dx = -\int_0^1 \frac{\partial^2}{\partial x^2}\left(K1(x)\ \frac{\partial^2 W(x)}{\partial x^2}\right) W^*(x,s)dx$$
$$-\int_0^1 K2(x)\,\ddot{W}(x)W^*(x,s)dx -$$
$$\int_0^1 \kappa^*(x)W(x)W^*(x,s)dx - \lambda^*\int_0^1 \frac{\partial^2 W}{\partial x^2}W^*(x,s)dx + \int_0^1 p^*(x)W^*(x,s)dx \tag{11}$$

$$\begin{cases} \int_0^1 \frac{\partial^4 W}{\partial x^4}(x) W^*(s,x)dx = W(s) + A0(s) \\ A0(s) = \left[W^*(s,x)\frac{\partial^3 W}{\partial x^3}(x) - \frac{\partial W^*}{\partial x}(s,x)\frac{\partial^2 W}{\partial x^2}(x) + \frac{\partial^2 W^*}{\partial x^2}(s,x)\theta(x) - \frac{\partial^3 W^*}{\partial x^3}(s,x)W(x) \right]_0^1 \end{cases} \quad (12)$$

Transverse displacement $W(x,\tau)$ in the right hand side of (11) is assumed to be:

$$W(x,\tau) = \sum_{j=1}^{n+2} \alpha_j(\tau) \cdot f_j(x) \quad (13)$$

where α_j are the amplitude coefficients and f_j are radial basis functions. Given f_j defines three other functions g_j, h_j and l_j which satisfy:

$$\frac{d^4 g_j}{dx^4}(x) = f_j(x),\ \frac{d^2 l_j}{dx^2}(x) = K1(x)\frac{d^2 f_j}{dx^2}(x) \text{ and } \frac{d^4 h_j}{dx^4}(x) = K2(x)\, f_j(x) \quad (14)$$

Explicit expressions of these functions are given in Appendix. Using (13) and (14), the rhs terms of (11) are expressed as:

$$\begin{cases} -\int_0^1 \frac{\partial^2}{\partial x^2}\left(K1(x)\ \frac{\partial^2 W(x)}{\partial x^2}\right) W^*(x,s)dx = \\ -\sum_{j=1}^{n+2}\alpha_j(\tau)\int_0^1 \frac{\partial^2}{\partial x^2}\left(K1(x)\frac{\partial^2 f_j}{\partial x^2}(x)\right) W^*(x,s)dx \\ \quad = -\sum_{j=1}^{n+2}\alpha_j(\tau)\int_0^1 \frac{\partial^4 l_j}{\partial x^4}(x) W^*(x,s)dx \\ \quad = -\sum_{j=1}^{n+2}\alpha_j(\tau) A_j(s) \\ A_j(s) = l_j(s) + \left[W^*(s,x)\frac{d^3 l_j}{dx^3}(x) - \frac{\partial W^*}{\partial x}(s,x)\frac{d^2 l_j}{dx^2}(x) + \frac{\partial^2 W^*}{\partial x^2}(s,x)\frac{dl_j}{dx}(x) - \frac{\partial^3 W^*}{\partial x^3}(s,x) l_j(x) \right]_0^1 \end{cases} \quad (15)$$

$$\begin{cases} -\int_0^1 K2(x)\ddot{W}(x)W^*(s,x)dx = -\sum_{j=1}^{n+2}\left(\ddot{\alpha}_j\ M1_j(s)\right) \\ M1_j(s) = h_j(s) + \left[W^*(s,x)\frac{d^3 h_j}{dx^3}(x) - \frac{\partial W^*}{\partial x}(s,x)\frac{d^2 h_j}{dx^2}(x) + \frac{\partial^2 W^*}{\partial x^2}(s,x)\frac{dh_j}{dx}(x) - \frac{\partial^3 W^*}{\partial x^3}(s,x)h_j(x) \right]_0^1 \end{cases} \quad (16)$$

$$\begin{cases} -\lambda^* \int_0^1 \frac{\partial^2 W}{\partial x^2} W^*(x,s)dx = -\lambda^* \sum_{j=1}^{n+2}\int_0^1 \alpha_j \frac{\partial^2 f_j}{\partial x^2}(x) W^*(s,x)dx \\ \quad = -\lambda^* \sum_{j=1}^{n+2}\alpha_j F_j(s) \\ F_j(s) = \frac{\partial^2 g_j}{\partial x^2}(s) + \left[W^*(s,x)\frac{d^5 g_j}{dx^5}(x) - \frac{\partial W^*}{\partial x}(s,x)\frac{d^4 g_j}{dx^4}(x) + \frac{\partial^2 W^*}{\partial x^2}(s,x)\frac{d^3 g_j}{dx^3}(x) - \frac{\partial^3 W^*}{\partial x^3}(s,x)\frac{d^2 g_j}{dx^2}(x) \right]_0^1 \end{cases} \quad (17)$$

For a concentrated elastic foundation κ^* at point x_k:

$$\begin{cases} -\int_0^1 \kappa^*(x)\left(W(x)\delta(x-x_k)\right)W^*(s,x)dx = \\ \quad -\kappa^*(x_k)W(x_k)W^*(s,x_k) \\ \quad = -\kappa^* \sum_{j=1}^{n+2} W_j L_j(s) \\ L_j(s) = 0 \quad j \neq k; L_k(s) = W^*(s,x_k), j \neq k \end{cases} \quad (18)$$

$$\int_0^1 p^*(x)W^*(x,s)dx = P(s) \quad (19)$$

For a compact equation representation, let us recall that in bending problem of beams, the following variable have physical meaning and may be known at boundaries.

$$\theta(x) = \frac{\partial W}{\partial x},\quad M(x) = -K_1(x)\frac{\partial^2 W}{\partial x^2} \text{ and } Q(x) = \frac{\partial M}{\partial x} \quad (20)$$

where $\theta(x)$ is slop, $Mo(x)$ is bending moment and $Q(x)$ is shear force, related to derivatives of deflection W. These physical parameters will be combined with W-equations and boundary conditions in order to get a well posed problem.

III. Matrix Formulation

For simplified expressions, the following notations are introduced:

$$\hat{J}(s) = \frac{\partial J}{\partial s}(s),\quad \hat{\hat{J}}(s) = K1(s)\cdot\frac{\partial \hat{J}}{\partial s}(s) \text{ and } \hat{\hat{\hat{J}}}(s) = \frac{\partial \hat{\hat{J}}}{\partial s}(s) \quad (21)$$

Based on these notations, the integral equation formulation (11) is reduced to the following algebro-differential equation at interior points:

$$W(s) + A0(s) = -\sum_{j=1}^{n+2}\left\{ \ddot{\alpha}_j\ M1_j(s) + \kappa^*\ W_j\ L_j(s) + \alpha_j\left(\left[\lambda^* F_j(s)\right] + \left[A_j(s)\right]\right)\right\} + \mathrm{P}(s) \quad (22)$$

In order to present a well posed problem in its general formulation, more equations than (22) related to θ, Mo and Q

are needed. They are obtained by the derivative of (22). The slope equation given by:

$$\theta(s)+\hat{A}0(s)=-\sum_{j=1}^{n+2}\left\{\begin{array}{l}\ddot{\alpha}_j\ \hat{M}1_j(s)+\kappa^*\ W_j\ \hat{L}_j(s)+\\ +\alpha_j\left(\left[\lambda^*\hat{F}_j(s)\right]+\left[\hat{A}_j(s)\right]\right)\end{array}\right\}+\hat{\mathrm{P}}(s) \tag{23}$$

For numerical results, discretization of beam is necessary. This discretization may be uniform or non uniform in order to improve the accuracy in case of a concentrated source of density. After discretization and using following notations, we get:

$$\left\{\begin{array}{l} W_i+A0_i=-\sum_{j=1}^{n+2}\left\{\begin{array}{l}\ddot{\alpha}_j\ M1_{ij}+\kappa^*\ W_j\ L_{ij}+\\ \alpha_j\left(\left[\lambda^*F_{ij}\right]+\left[A_{ij}\right]\right)\end{array}\right\}+\mathrm{P}_i \\ \theta_i+\hat{A}0_i=-\sum_{j=1}^{n+2}\left\{\begin{array}{l}\ddot{\alpha}_j\ \hat{M}1_{ij}+\kappa^*\ W_j\ \hat{L}_{ij}+\\ \alpha_j\left(\left[\lambda^*\hat{F}_{ij}\right]+\left[\hat{A}_{ij}\right]\right)\end{array}\right\}+\hat{\mathrm{P}}_i \\ \qquad i=1;n+2 \end{array}\right. \tag{24}$$

in which $W_i=W(s_i)$, $s_i=i-1/n+1$, *i=1* and *i=n+2* correspond to the beam ends and *i=2* to *n+2* correspond to interior points. This system of equation contains both unknowns at interiors points and boundaries.

A. Generalized Boundary Conditions

A non uniform beam with circular cross section is considered. Fixations are generalized by the introduction of linear and rotary springs at the two ends of the beams. Linear fixations and follower force acts on the shear force whereas rotary fixations affect the moment. For the used sections, boundary conditions at beam ends *i=1* and *i= n+2* are [6], [10]:

$$\left\{\begin{array}{l}\left(1+K1(0)\right)\dfrac{\partial^2W}{\partial x^2}(0)=\kappa^*_{r0}\ \theta_1\ , \\ \left(1+K1(1)\right)\dfrac{\partial^2W}{\partial x^2}(1)=\kappa^*_{r1}\ \theta_{n+2} \\ \dfrac{d}{dx}\left(\left(1+K1(x)\right)\dfrac{\partial^2W}{\partial x^2}\right)(0)=-\kappa^*_{l0}W_1+(1-y)\lambda^*\theta_1 \\ \dfrac{d}{dx}\left(\left(1+K1(x)\right)\dfrac{\partial^2W}{\partial x^2}\right)(1)=-\kappa^*_{l1}W_{n+2}+(1-y)\lambda^*\theta_{n+2}\end{array}\right. \tag{25}$$

as $K1(0)=0$, (25) can be rewritten as:

$$\left\{\begin{array}{l}\dfrac{\partial^2W}{\partial x^2}(0)=\kappa^*_{r0}\ \theta_1\ ,\quad \dfrac{\partial^2W}{\partial x^2}(1)=\dfrac{\kappa^*_{r1}}{\left(1+K1(1)\right)}\theta_{n+2} \\ \dfrac{\partial^3W}{\partial x^3}(0)=-\kappa^*_{l0}W_1+\left((1-y)\lambda^*-\dfrac{dK1}{dx}(0)\kappa^*_{r0}\right)\theta_1 \\ \dfrac{\partial^3W}{\partial x^3}(1)=-\dfrac{\kappa^*_{l1}}{\left(1+K1(1)\right)}W_{n+2}+ \\ +\left(\dfrac{(1-y)}{\left(1+K1(1)\right)}\lambda^*-\dfrac{dK1}{dx}(1)\dfrac{\kappa^*_{r1}}{\left(1+K1(1)\right)^2}\right)\theta_{n+2}\end{array}\right. \tag{26}$$

By putting (26) into (12), we get:

$$\begin{aligned} A0(s)=&\underbrace{\left(\frac{\partial^3W^*}{\partial x^3}(s,0)+\kappa^*_{l0}W^*(s,0)\right)}_{R1(s)}W_1+\\ &\underbrace{-\left(\frac{\partial^3W^*}{\partial x^3}(s,1)+\frac{\kappa^*_{l1}}{\left(1+K1(1)\right)}W^*(s,1)\right)}_{R2(s)}W_{n+2}+\\ &\underbrace{+\left(\begin{array}{l}-\dfrac{\partial^2W^*}{\partial x^2}(s,0)+\kappa^*_{r0}\dfrac{\partial W^*}{\partial x}(s,0)+\\ \kappa^*_{r0}\dfrac{dK1}{dx}(0)W^*(s,0)\end{array}\right)}_{R3(s)}\theta_1+\\ &\underbrace{(1-y)\lambda^*\left(-W^*(s,0)\theta_1+\frac{W^*(s,1)}{\left(1+K1(1)\right)}\theta_{n+2}\right)}_{F0(s)}+\\ &\underbrace{+\left(\begin{array}{l}\dfrac{\partial^2W^*}{\partial x^2}(s,1)-\dfrac{\kappa^*_{r1}}{\left(1+K1(1)\right)}\dfrac{\partial W^*}{\partial x}(s,1)-\\ \kappa^*_{r1}\dfrac{dK1}{dx}(1)\dfrac{W^*(s,1)}{\left(1+K1(1)\right)^2}\end{array}\right)}_{R4(s)}\theta_{n+2}\end{aligned} \tag{27}$$

By this way, the considered boundary conditions are taken into account in present formula. Equation (11) becomes more compact as:

$$\left\{\begin{array}{l}A0(s)=\underbrace{R1(s)\ W_1+R2(s)\ W_{n+2}+}_{R(s)}\\ \qquad\underbrace{+R3(s)\ \theta_1+R4(s)\ \theta_{n+2}}\\ \qquad+\lambda^*(1-y)F0(s)\\ \hat{A}0(s)=\hat{R}(s)+\lambda^*(1-y)\hat{F}0(s)\end{array}\right. \tag{28}$$

Or in a discretized form:

$$\left\{\begin{array}{l}A0_i=R_i+\lambda^*(1-y)\hat{F}0_i,\quad i=1\ \text{to}\ n+2\\ \hat{A}0_i=\hat{R}_i+\lambda^*(1-y)\hat{F}0_i\end{array}\right. \tag{29}$$

By putting (29) into (24), leads to:

$$\left\{\begin{array}{ll} W_i+R_i+\lambda^*(1-y)\hat{F}0_i= & -\sum_{j=1}^{n+2}\left\{\ddot{\alpha}_j\ M1_{ij}+\kappa^*W_jL_{ij}+\alpha_j\left(\left[\lambda^*F_{ij}\right]+\left[A_{ij}\right]\right)\right\}+\\ +\mathrm{P}_i, & i=1\ \text{to}\ n+2\\ \theta_i+\hat{R}_i+\lambda^*(1-y)\hat{F}0_i= & -\sum_{j=1}^{n+2}\left\{\ddot{\alpha}_j\ \hat{M}1_{ij}+\kappa^*W_j\hat{L}_{ij}+\alpha_j\left(\left[\lambda^*\hat{F}_{ij}\right]+\left[\hat{A}_{ij}\right]\right)\right\}+\\ +\hat{\mathrm{P}}_i, & i=1\ \text{and}\ i=n+2\end{array}\right. \tag{30}$$

Finally, we have '*n+2*' equations by applying the first equation of (30) and '*n+4*' unknowns ('*n+2*' unknowns of W_i, θ_1 and θ_{n+2}). The two additional equations can be explicitly expressed by applying the second equation of (30). The well posed system of equations is formulated by '*n+4*' equations:

- *'n+2'* equations by applying the first equation of (30), *i=1 to n+2*,
- 2 additional equations by applying the second equation of (30), *i=1* and *i=n+2*.

B. Global System

In order to formulate the system of equations, we apply deflection equation for all points of the beam (the first equation of (30) for *i=1 to n+2*) and bending equations at the ends of the beam (the second equation of (30) for *i=1* and *i=n+2*). We get:

$$\begin{cases} W_1+R_1=-\sum_{j=1}^{n+2}\alpha_j A_{1j}-\sum_{j=1}^{n+2}\ddot{\alpha}_j M1_{1j}- \\ \qquad \kappa^*\sum_{j=1}^{n+4}W_j L_{1j}-\lambda^*\sum_{j=1}^{n+4}\alpha_j F_{1j}- \\ \qquad \lambda^*(1-y)\sum_{j=1}^{n+4}W_j F0_{1j}+\mathrm{P}_1; \quad i=1 \\ \vdots \qquad\qquad \vdots \qquad\qquad \vdots \\ \underbrace{W_i}_{[\mathbf{I}]\{W\}}+\underbrace{R_i}_{[\mathbf{R}]\{W\}}=\underbrace{-\sum_{j=1}^{n+2}\alpha_j A_{ij}}_{[\mathbf{A}][\mathbf{G}]\{W\}}\underbrace{-\sum_{j=1}^{n+2}\ddot{\alpha}_j M1_{ij}}_{[\mathbf{M1}][\mathbf{G}]\{\ddot{W}\}}- \\ \qquad \underbrace{\kappa^*\sum_{j=1}^{n+4}W_j L_{ij}}_{\mu^*[\mathbf{L}]\{\ddot{W}\}}\underbrace{-\lambda^*\sum_{j=1}^{n+4}\alpha_j F_{ij}}_{\lambda^*[\mathbf{F}][\mathbf{G}]\{W\}}\underbrace{-\lambda^*(1-y)\sum_{j=1}^{n+4}W_j F0_{ij}}_{\lambda^*[\mathbf{F0}]\{W\}}+\underbrace{\mathrm{P}_i}_{\{P\}} \\ \vdots \qquad\qquad \vdots \qquad\qquad \vdots\, i=n+2 \\ \theta_1+\hat{R}_1=-\sum_{j=1}^{n+2}\alpha_j \hat{A}_{1j}-\sum_{j=1}^{n+2}\ddot{\alpha}_j \hat{M}1_{1j}-\kappa^*\sum_{j=1}^{n+4}W_j \hat{L}_{1j}- \\ \qquad \lambda^*\sum_{j=1}^{n+4}\alpha_j \hat{F}_{1j}-\lambda^*(1-y)\sum_{j=1}^{n+4}W_j \hat{F}0_{1j}+\hat{\mathrm{P}}_1;\ i=1 \\ \theta_{n+2}+\hat{R}_{n+2}=-\sum_{j=1}^{n+2}\alpha_j \hat{A}_{n+2,j}-\sum_{j=1}^{n+2}\ddot{\alpha}_j \hat{M}1_{n+2,j}- \\ \qquad \kappa^*\sum_{j=1}^{n+4}W_j \hat{L}_{n+2,j}-\lambda^*\sum_{j=1}^{n+4}\alpha_j \hat{F}_{n+2,j}- \\ \qquad \lambda^*(1-y)\sum_{j=1}^{n+4}W_j \hat{F}0_{n+2,j}+\hat{\mathrm{P}}_{n+2,j}; \qquad i=n+2 \end{cases} \tag{31}$$

For the sake of clarity, this equation is rewritten in a more compact matrix form as:

$$[\mathbf{M}]\{\ddot{W}\}+[\mathbf{K}]\{W\}=\{P\} \tag{32}$$

in which: $[\mathbf{M}]=[\mathbf{M1}][\mathbf{G}]$;

$$[\mathbf{K}]=[\mathbf{I}]+[\mathbf{R}]+\kappa^*[\mathbf{L}]+[\mathbf{A}][\mathbf{G}]+\lambda^*([\mathbf{F}][\mathbf{G}]+(1-y)[\mathbf{F0}]); \tag{33}$$
$$\{W\}=\{W_1,W_2,W_3,\cdots,W_{n+1},W_{n+2},\theta_1,\theta_{n+2}\}$$

$[\boldsymbol{M}]$ or $[\boldsymbol{K}]$ are mass and rigidity matrices. The presented formula of the matrix $[\boldsymbol{K}]$ helps us to see effect of foundation, load and sub-tangential load angle clearly. These matrices are explicitly given in appendix B. Numerical solution of (32) allows us to investigate buckling, vibration and flutter of beams with variable cross sections under generalized boundary conditions.

IV. Eigenvalue Procedure

A. Buckling Problem

Buckling problem may be formulated by assuming static displacements and omitting excitation and sub-tangential parameters in (32). The critical buckling loads and associated eigenmodes can be determined for various types of boundary conditions and concentrated elastic foundation κ^* by solving following eigenvalue problem:

$$\begin{cases} [\mathbf{X}]\{W\}=\dfrac{1}{\lambda_c^*}\{W\} \\ [\mathbf{X}]=-\left([\mathbf{I}]+[\mathbf{R}]+\kappa^*[\mathbf{L}]+[\mathbf{A}][\mathbf{G}]\right)^{-1}[\mathbf{F}][\mathbf{G}] \end{cases} \tag{34}$$

This allows the investigation of numerical critical buckling loads and associated eigenmodes at interior points. The corresponding slope, moment and shear force can be numerically computed using following relationships:

$$\begin{cases} \{\theta\}=-\left([\hat{\mathbf{R}}]+\kappa^*[\hat{\mathbf{L}}]+[\hat{\mathbf{A}}]-\lambda_c^*[\hat{\mathbf{F}}][\mathbf{G}]\right)\{W\}_i \\ \{Mo\}=[\mathbf{diag}(\mathbf{1}+\mathbf{K1_i})]\left(\begin{matrix}[\hat{\mathbf{R}}]+\kappa^*[\hat{\mathbf{L}}]+[\hat{\hat{\mathbf{A}}}]+ \\ -\lambda_c^*[\hat{\hat{\mathbf{F}}}][\mathbf{G}]\end{matrix}\right)\{W\}_i \\ \{Q\}=\left\{\begin{matrix}\left[\mathbf{diag}\left(\dfrac{\hat{\mathbf{K1_i}}}{\mathbf{1}+\mathbf{K1_i}}\right)\right]+ \\ +[\mathbf{diag}(\mathbf{1}+\mathbf{K1_i})]\left(\begin{matrix}[\hat{\hat{\mathbf{R}}}]+\kappa^*[\hat{\hat{\mathbf{L}}}]+ \\ +[\hat{\hat{\hat{\mathbf{A}}}}]-\lambda_c^*[\hat{\hat{\hat{\mathbf{F}}}}][\mathbf{G}]\end{matrix}\right)\end{matrix}\right\}\{W\}_i \end{cases} \tag{35}$$

In which λ_c^* is the i^{th} critical buckling load associated to the i^{th} buckling mode shape $\{W\}_i$.

B. Flutter Problem

Let us assume that displacement field can be written in the following form:

$$W(x,\tau)=W(x)\,e^{\Omega^*\tau}, \qquad \Omega^*=\alpha^*+\omega^* i \tag{36}$$

Numerical solution of (32) permits, on one hand, to study linear vibration behaviors of beams by omitting the load parameter. On the other hand, linear vibration analysis of beams under axial compression and instability phenomenon can be investigated by numerically solving the following eigenvalue problem for each fixed load parameter:

$$\begin{cases} [\mathbf{X}]\ \{W\} = \dfrac{1}{\Omega^{*2}}\{W\} \\ [\mathbf{X}] = -\left(\begin{matrix} [\mathbf{I}] + [\mathbf{R}] + \kappa^{*}[\mathbf{L}] + [\mathbf{A}][\mathbf{G}] + \\ + \lambda^{*}([\mathbf{F}][\mathbf{G}] + (1-y)[\mathbf{F0}]) \end{matrix} \right)^{-1} [\mathbf{M}] \end{cases} \quad (37)$$

Remember that matrix $[\mathbf{X}]$ is λ^{*} and 'y' dependent and is particularly not symmetric. Generalized boundary conditions are expressed by the $[\boldsymbol{R}]$ matrix. The load-frequency dependence can be investigated and the divergence stability may be analyzed for various modulus and position of elastic foundation. This system includes all considered parameters and represents a general formulation for computing corresponding physical parameters (slope, moment and shear force) required for designers without more computation effort.

$$\begin{cases} \{\theta\} = -\left(\begin{matrix} [\hat{\mathbf{R}}] + \kappa^{*}[\hat{\mathbf{L}}] + [\hat{\mathbf{A}}] + \\ + \lambda^{*}([\hat{\mathbf{F}}][\mathbf{G}] + (1-y)[\hat{\mathbf{F}}\mathbf{0}]) - \Omega_i^{*2}[\hat{\mathbf{M}}] \end{matrix} \right) \{W\}_i \\ [\mathbf{Mo}] = [\mathbf{diag}(\mathbf{1} + \mathbf{K1_i})] \ . \\ . \left(\begin{matrix} [\hat{\hat{\mathbf{R}}}] + \kappa^{*}[\hat{\hat{\mathbf{L}}}] + [\hat{\hat{\mathbf{A}}}] + \\ + \lambda^{*}\left([\hat{\hat{\mathbf{F}}}][\mathbf{G}] + (1-y)[\hat{\hat{\mathbf{F}}}\mathbf{0}] \right) - \Omega_i^{*2}[\hat{\hat{\mathbf{M}}}] \end{matrix} \right) \{W\}_i \\ [\mathbf{Q}] = \left[\mathbf{diag}\left(\dfrac{\hat{\mathbf{K1}}_{\mathbf{i}}}{\mathbf{1} + \mathbf{K1_i}} \right) \right] [\mathbf{Mo}] - [\mathbf{diag}(\mathbf{1} + \mathbf{K1_i})] \ . \\ . \left\{ \omega_i^{*2}[\hat{\hat{\hat{\mathbf{M}}}}]\{W\}_i + \right. \\ \left. + \left(\begin{matrix} [\hat{\hat{\hat{\mathbf{R}}}}] + \kappa^{*}[\hat{\hat{\hat{\mathbf{L}}}}] + [\hat{\hat{\hat{\mathbf{A}}}}] + \\ \lambda^{*}\left([\hat{\hat{\hat{\mathbf{F}}}}][\mathbf{G}] + (1-y)[\hat{\hat{\hat{\mathbf{F}}}}\mathbf{0}] \right) - \Omega_i^{*2}[\hat{\hat{\hat{\mathbf{M}}}}] \end{matrix} \right) \{W\}_i \right\} \end{cases} \quad (38)$$

where $\omega_i^{*} = \mathrm{fct}(\lambda^{*}, y)$ is the i^{th} natural frequency associated to the i^{th} vibration mode $\{W\}_i = \mathrm{fct}(\lambda^{*}, y)$.

V. Numerical Results

The present mathematical formula is developed for a non uniform beam subjected to a non conservative force. Boundary conditions are represented by the generalized fixations parameterized by linear and rotary springs to deal with various and realistic types of fixations. In this paper, the analysis concerns slender beams with linear variation and circular cross section. Extension to other types of sections can be easily done. Critical buckling loads and natural frequencies and corresponding eigenmodes can be determined by solving the resulting eigenvalue problem at concatenation points. Deflection, slope, bending moment and shear force can be also investigated at interior and boundaries of beam. The accuracy of the result increases with the number of interior points and 40 points seem to be enough. Many types of beams are analyzed in order to demonstrate the effectiveness of the developed approach.

A. Nonuniform Beam

1. Influence of the Elastic Fixation Parameters on the Natural Frequencies

Considering a beam with linear variation and circular cross section for which taper ratio is $r = d_1/d_0$ (Figs. 3 (a) and (b)). In practice, ideal fixation does not exist and then the parameterization of the fixations is more realistic. Based on the presented formulations, the five natural frequencies according to the linear and rotary stiffness coefficient κ_{10}^{*} and κ_{r0}^{*} for the first end fixation ($x=0$) and κ_{11}^{*} and κ_{r1}^{*} for the second end fixation ($x=1$) are given in Tables I and II. Obtained results by 40 internal points are well compared to [1] using Bessel functions. It is demonstrated from these tables that boundary stiffness fixations may largely influence vibration behaviors of the beam. Classical boundary conditions such as simply supported ($\kappa_1^{*} = \infty$ and $\kappa_r^{*} = 0$) and clamped ($\kappa_1^{*} = \infty$, $\kappa_r^{*} = \infty$) are also modeled by these fixations. These generalized boundary conditions are more realistic and allow us to investigate the imperfections in the boundary conditions. The stiffness parameters have a strong influence as shown in Tables I and II.

2. Influence of the Taper Ratio on the Natural Frequencies and the Mode Shapes

Influence of taper ratio '*r*' on the mode shapes is shown in Figs. 4-9 for simply supported-clamped (C-S) beam and in Figs. 10-13 for a cantilever beam (C-F). The lowest five mode shapes for different values of 'r' are presented. We notice that amplitude of the mode decreases with increasing section. This is due to the fact that rigidity of beam increases with section. The influence of taper ratio '*r*' on the first fifth natural frequencies is given in Table III for a C-S beam. Effect of '*r*' tends to increase natural frequencies modulus of the C-S beam. Let us note that for '$r > 1$' there is a critical value r_c of taper ratio for which the first and the second frequencies become complex conjugate. This means that for $r > r_c$, beam will flutter even if no charge acts on it. This critical value r_c, depending on the boundary conditions considered, is of great importance for a safe design.

B. Dynamic Instability of a Chimney

Our aim in this subsection is to give an industrial application of the present model. A case studied here corresponds to an industrial realistic chimney (OCP, Morocco) which is very long in order to drain the toxic gas at a very high altitude [11]. This chimney can be assimilated and approximated by a non uniform slender C-F tube with linear variation and constant thickness along the longitudinal axis. The corresponding approximated geometrical and material characteristics are given in Table IV. The vibration analysis of this chimney is investigated and the two first natural frequencies of the considered C-F chimney are given in Table V for various taper ratios r. It is demonstrated that there is a critical r_c ($r_c = 1.045$) under which the chimney becomes

instable and will flutter. From these results, it appears that a deep investigation of this critical value related to boundary conditions and geometrical parameters is necessary for safe design of chimneys. For flutter analysis, the chimney is assumed to be submitted to a sub-tangential follower force ($y=1$). Load-frequency dependence is investigated and flutter phenomenon is analyzed for different values of taper ratio 'r' using the coalescence criterion. The obtained load frequency curves are presented in Figs. 14-18. These figures show a higher dependence between flutter load and taper ratio. The dynamic analysis of the chimney shows first that, for $r < r_c$ ($r_c=1.045$, Table V), the flutter load increases with increasing taper ratio 'r' as shown in Figs. 14-18. Chimney will flutter when the non conservative load exceed flutter load value. For a uniform chimney ($r=1$), flutter curve is presented in Figs. 14-17 for comparison and flutter load is $\lambda^*_{flutter} \approx 16 \text{ x } 10^5 N$. For $r=0.5$, the chimney will first diverge at $\lambda^*_d \approx 42 \text{ x } 10^5 N$ and then flutter at $\lambda^*_{flutter} \approx 81 \text{ x } 10^5 N$. For $r=0.1$, the flutter load $\lambda^*_{flutter}$ is $8 \text{ x } 10^7 N$. These values demonstrate that the chimney with a large basis is more stable than the one with a reduced basis. A deep analysis of dynamic behavior of this chimney is given in Fig. 18 for refined values of 'r'. it is shown that around the critical value $r_c=1.045$, dynamic behavior is strongly affected and in some cases the chimney has to be loaded in order to be stabilized.

VI. Conclusion

A methodological approach based on integral equation formulations for dynamic analysis of a non uniform slender beam subjected to a sub-tangential follower force and generalized boundary conditions is presented in simple and compact forms. Required matrices are explicitly given and dynamic analysis is be investigated by solving the resulting eigenvalue problems. The coalescence criterion was used for flutter analysis and many numerical tests are performed. The effect of taper ratio on the natural frequencies, flutter loads and mode shapes is investigated for non-uniform beams and chimneys. The presented model is quite general and obtained results are in agreement with available data. These investigations demonstrated the effectiveness of the developed methodological approach.

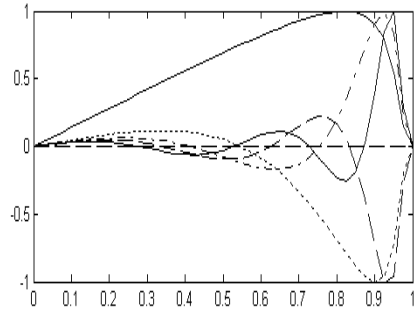

Fig. 4 The lowest five mode shapes for a non uniform S-C beam for $r=0.0001$

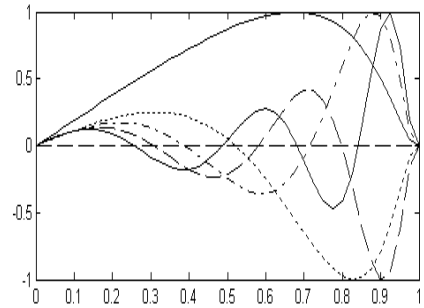

Fig. 5 The lowest five mode shapes for a non uniform S-C beam for $r=0.1$

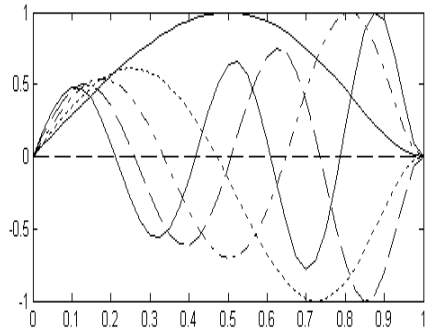

Fig. 6 The lowest five mode shapes for a non uniform S-C beam for $r=0.5$

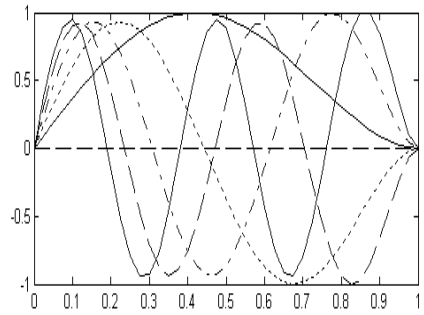

Fig. 7 The lowest five mode shapes for a non uniform S-C beam for $r=1$

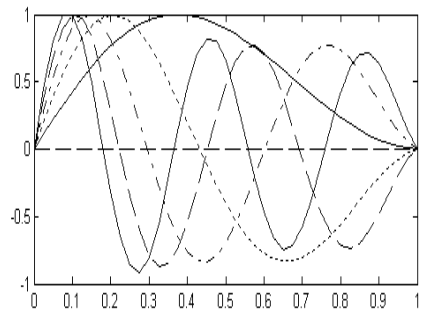

Fig. 8 The lowest five mode shapes for a non uniform S-C beam for $r=1.5$

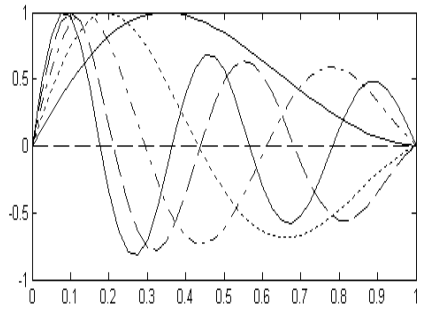

Fig. 9 The lowest five mode shapes for a non uniform S-C beam for *r=2*

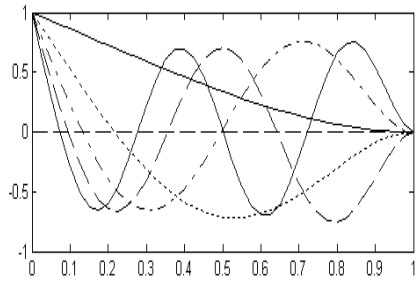

Fig. 10 The lowest five mode shapes for a non uniform F-C beam for *r=1*

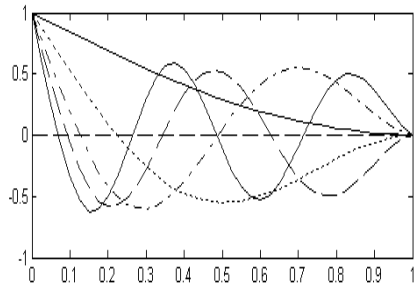

Fig. 11 The lowest five mode shapes for a non uniform F-C beam for *r=1.5*

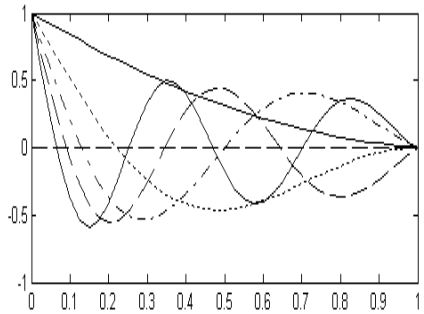

Fig. 12 The lowest five mode shapes for a non uniform F-C beam for *r=2*

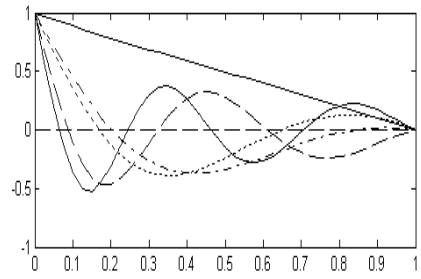

Fig. 13 The lowest five mode shapes for a non uniform F-C beam for *r=1*

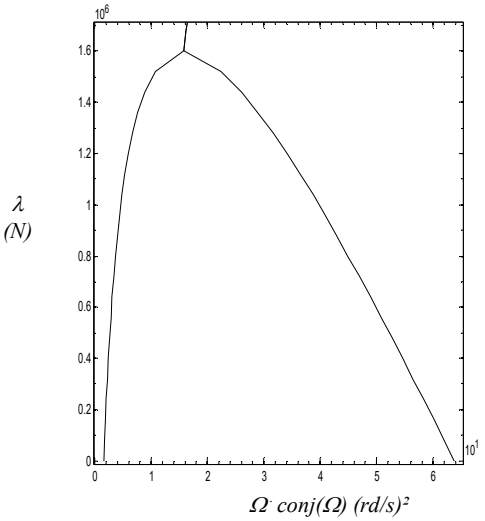

Fig. 14 The load-frequency curve for a non uniform slender C-F beam for *r=1, λf=1.6* x *10^6 N*

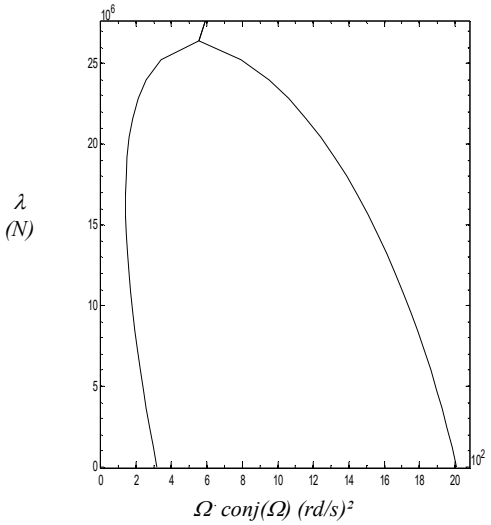

Fig. 15 The load-frequency curve for a non uniform slender C-F beam for *r=0.2, λf=27* x *10^6 N*

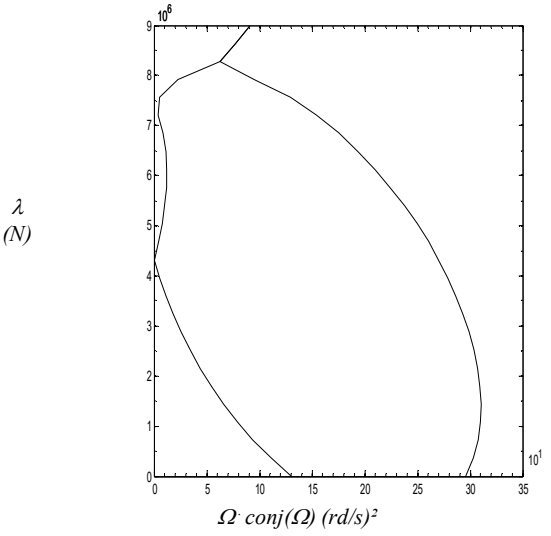

Fig. 16 The load-frequency curve for a non uniform slender C-F beam for $r=0.5$, $\lambda d=4.2$ x 10^6 N, $\lambda f=8.3$ x 10^6 N

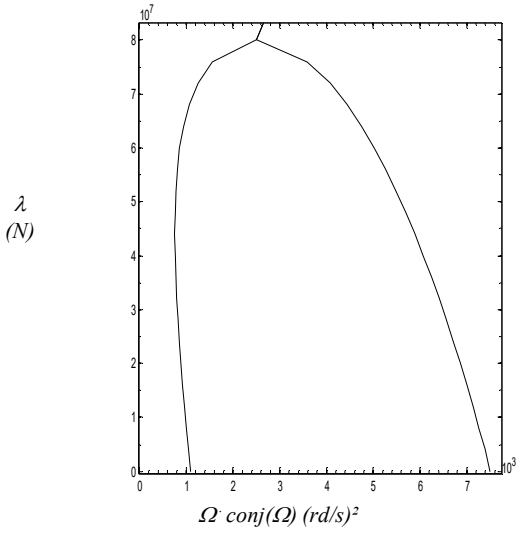

Fig. 17 The load-frequency curve for a non uniform slender C-F beam for $r=0.1$, $\lambda f=8.7$ x 10^7 N

TABLE I
THE FIVE LOWEST NATURAL FREQUENCIES (ω^*) OF A NON UNIFORM CIRCULAR BEAM FOR $\kappa_{l0}^* = \kappa_{l1}^* = \infty$ AND $R=2$, FOR VARIOUS VALUES OF THE NON DIMENSIONAL ROTATIONAL STIFFNESS COEFFICIENTS κ_{r0}^* AND κ_{r1}^* OBTAINED BY THE PRESENT MODEL ($N=40$) AND COMPARED TO [1]

	Natural Frequencies ω^*					
	$\kappa_{r0}^*=0$	$\kappa_{r1}^*=0$	$\kappa_{r0}^*=1$	$\kappa_{r1}^*=1$	$\kappa_{r0}^*=0$	$\kappa_{r1}^*=10$
I	*Model [1]*	*Present* Model	*Model [1]*	*Present* Model	*Model [1]*	*Present* Model
1	13.91	14.04	9.73	9.10	22.56	18.11
2	58.22	51.40	61.00	51.47	68.56	45.25
3	130.42	114.42	133.71	117.97	142.32	126.53
4	231.04	250.62	234.09	239.52	243.98	231.25
5	360.62	311.77	363.66	328.60	374.42	342.02

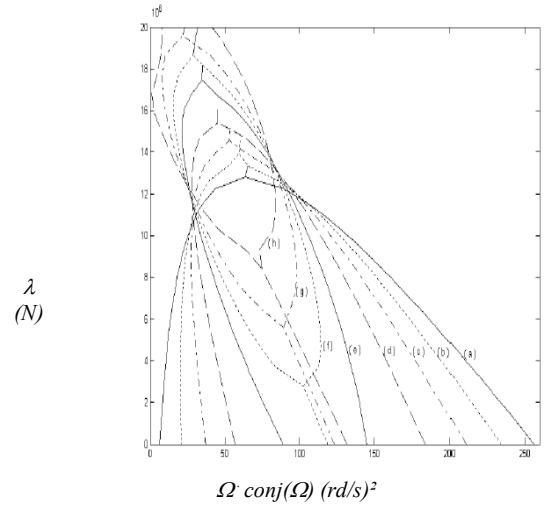

Fig. 18 The load-frequency curve for a non uniform slender C-F beam for different values of ratio $r>1$: *(a): r=1, (b): r=1.01, (c): r=1.02, (d): r=1.03, (e): r=1.04, (f): r=1.045, (g): r=1.056, (h): r=1.06*

TABLE II
THE FIVE LOWEST NATURAL FREQUENCIES (ω^*) OF A NON UNIFORM CIRCULAR BEAM FOR $\kappa_{r1}^* = \kappa_{l1}^* = \infty$ AND $R=1.4$, FOR VARIOUS VALUES OF THE NON DIMENSIONAL ROTATIONAL AND LINEAR STIFFNESS COEFFICIENTS κ_{r0}^* AND κ_{l0}^* OBTAINED BY THE PRESENT MODEL ($N=40$) AND COMPARED TO [1]

	Natural Frequencies ω^*					
	$\kappa_{r0}^*=0$	$\kappa_{l0}^*=\infty$	$\kappa_{r0}^*=0$	$\kappa_{l0}^*=10^3$	$\kappa_{r0}^*=0$	$\kappa_{l0}^*=0$
I	*Model [1]*	*Present* Model	*Model [1]*	*Present* Model	*Model [1]*	*Present* Model
1	19.62	19.53	19.18	19.01	5.66	3.65
2	60.84	59.95	55.95	55.62	28.84	28.98
3	125.44	124.02	104.45	102.78	76.21	73.70
4	231.74	211.24	165.38	164.96	146.65	145.81
5		320.55		246.83		236.23

TABLE III
THE FIVE LOWEST NATURAL FREQUENCIES (Ω^*) OF A NON UNIFORM CIRCULAR C-S BEAM FOR VARIOUS VALUES OF THE RATIO R. ($\lambda^* = 0$)

	Natural Frequencies ω^*					
i	*r=0.1*	*r=0.5*	*r=1*	*r= r_1=1.42*	*r=2*	*r=2.5*
1	10.31i	13.06i	15.41i	1.92 + 33.55i	30.77 + 34.44i	46.13 + 35.00i
2	27.40i	40.93i	49.96i	1.92 - 33.55i	30.77 - 34.44i	46.13 - 35.00i
3	53.01i	78.70i	104.24i	142.52 i	48.63 + 193.33i	77.64 + 218.04i
4	87.79i	138.25i	178.27i	184.68i	48.63 - 193.33i	77.64 - 218.04i
5	130.65i	203.21i	272.03i	344.72i	52.78 + 465.65i	93.72 + 530.71i

TABLE IV
GEOMETRICAL AND MATERIAL CHARACTERISTICS OF AN APPROXIMATED OCP MOROCCO CHIMNEY [11]

Length, L	*: 70 m*	*Inertia, I(0)*	*= 0.0491 m³*
Young Modulus, E	*: 2 x 10^{11}N/m²*	*Section, S(0)*	*= 0.7850 m²*
Mass density	*: 7847.03Kg/m³*	*Time coefficient, χ*	*= 3.8823 s*
Thickness	*: 5 mm*	*Gyration radius, R*	*= 0.25*
d_0	*: 2 m*		
d_1	*: 1 m*		

TABLE V
THE FIVE LOWEST NATURAL FREQUENCIES (Ω^*) OF A CHIMNEY FOR VARIOUS VALUES OF THE RATIO R (D_0=2)

	Natural Frequencies Ω (rd:/ s()						
i	*r=*	*r=*	*r=1*	*r=*	*r=*	*r=*	*r=*
	0.1	*0.5*		*1.04*	*1.045*	*1.05*	*1.1*
ω_1	0 + 4.571i	0 + 7.44i	0 + 1.81i	0 + 6.52i	0.69 + 7.66i	1.43 + 7.71i	3.82 + 8.01i
ω_2	0 +11.32i	0 + 11.58i	0 + 11.35i	0 + 8.70i	0.69 - 7.66i	1.43 - 7.71i	3.82 - 8.01i

APPENDIX

A. The Used Radial Basis Function

The fundamental solution W^* used in this analysis corresponds to $\frac{\partial^4}{\partial x^4}\left(W^*(x,s)\right)=\delta(x,s)$ is $W^*(x,s)=\frac{|x-s|^3}{12}$.

Several types of radial basis functions $f_j(x)$ are tested and the general form used is:

$$f_j(x)=a_0+a_1(x-xj)+a_2|x-xj|^2+a_3|x-xj|^3$$

$$\frac{d^4 g_j}{dx^4}(x)=f_j(x),\ \frac{d^2 l_j}{dx^2}(x)=K_1(x)\frac{d^2 f_j}{dx^2}(x) \text{ and}$$

$$\frac{d^4 h_j}{dx^4}(x)=K_2(x)\,f_j(x).$$

Then we have:

$$g_j(x)=\frac{a_0}{24}(x-xj)^4+\frac{a_1}{120}(x-xj)^5+\frac{a_2}{360}|x-xj|^6+\frac{a_3}{840}|x-xj|^7$$

The other functions $l_j(x)$ and $h_j(x)$ depend on the inertia and mass functions $K_1(x)$ and $K_2(x)$ chosen.

B. Used Matrices

$$[\mathbf{M}]\left\{\ddot{W}\right\}+\left([\mathbf{I}]+[\mathbf{R}]+\kappa^*[\mathbf{L}]+[\mathbf{A}][\mathbf{G}]+\right.$$
$$\left.+\lambda^*([\mathbf{F}][\mathbf{G}]+(1-y)[\mathbf{F0}])\right)\{W\}-\{P\}=0\ \ s_i=\frac{i-1}{n+1}$$

$[\mathbf{G1}]$: matrix ((n+2)x(n+2)) of radial basis functions

$$G1_{ij}=f_j(s_i),\ \ i=1,n+2\quad ;\ j=1,n+2$$

$[\mathbf{G}]$: matrix ((n+4)x(n+4))

$$G_{ij}=G1^{-1}{}_{i(j+1)}\quad i=1,n+2\quad ;\ \ j=1;n+2.$$

The other terms are null.

$[\mathbf{I}]$: Identity matrix ((n+4)x(n+4))

$[\mathbf{R}]$: matrix ((n+4)x(n+4))

$$\begin{cases} R_{i,1}=R1(s_i), \quad R_{i,n+2}=R2(s_i), \quad R_{i,n+3}=R3(s_i), \\ \quad R_{i,n+4}=R4(s_i). \quad i=1;n+2 \\ R_{n+3,1}=\hat{R}1(0), \quad R_{n+3,n+2}=\hat{R}2(0), \quad R_{n+3,n+3}=\hat{R}3(0), \\ \quad R_{n+3,n+4}=\hat{R}4(0). \\ R_{n+4,1}=\hat{R}1(1), \quad R_{n+4,n+2}=\hat{R}2(1), \quad R_{n+4,n+3}=\hat{R}3(1), \\ \quad R_{n+4,n+4}=\hat{R}4(1). \\ \text{the other terms are null} \end{cases}$$

$$\begin{cases} R1(s)=\frac{\partial^3 W^*}{\partial x^3}(s,0)+\kappa_{l0}^* W^*(s,0) \\ R2(s)=-\frac{\partial^3 W^*}{\partial x^3}(s,1)-\frac{\kappa_{l1}^*}{(1+K1(1))}W^*(s,1) \\ R3(s)=-\frac{\partial^2 W^*}{\partial x^2}(s,0)+\kappa_{r0}^*\frac{\partial W^*}{\partial x}(s,0)+\kappa_{r0}^*\frac{dK1}{dx}(0)W^*(s_i,0) \\ R4(s)=\frac{\partial^2 W^*}{\partial x^2}(s,1)-\frac{\kappa_{r1}^*}{(1+K1(1))}\frac{\partial W^*}{\partial x}(s,1)- \\ \qquad \kappa_{r1}^*\frac{dK1}{dx}(1)\frac{W^*(s_i,1)}{(1+K1(1))^2} \end{cases}$$

$[\boldsymbol{A}]$: matrix ((n+4)x(n+4)),

$$\begin{cases} A_{ij}=A_j(s_i). \quad i=1,n+2;\ j=1,n+2 \\ A_{n+3,j}=\hat{A}_j(0). \quad j=1,n+2 \\ A_{n+4,j}=\hat{A}_j(1). \quad j=1,n+2 \\ \text{the other terms are null} \end{cases}$$

$[\mathbf{M}]$: matrix ((n+4)x(n+4)), $[\mathbf{M}]=[\mathbf{M1}]\,[\mathbf{G}]$

$$\begin{cases} M1_{ij}=M1_j(s_i). \quad i=1,n+2;\ j=1,n+2 \\ M1_{n+3,j}=\hat{M}_j(0). \quad j=1,n+2 \\ M1_{n+4,j}=\hat{M}_j(1). \quad j=1,n+2 \\ \text{the other terms are null} \end{cases}$$

$[\mathbf{L}]$: matrix ((n+4)x(n+4)),

$$\begin{cases} L_{ij}=L_j(s_i). \quad i=1,n+2;\ j=1,n+2 \\ L_{n+3,j}=\hat{L}_j(0). \quad j=1,n+2 \\ L_{n+4,j}=\hat{L}_j(1). \quad j=1,n+2 \\ \text{the other terms are null} \end{cases}$$

$[\mathbf{F}]$: matrix ((n+4)x(n+4)),

$$\begin{cases} F_{ij}=F_j(s_i) \quad i=1,n+2;\ j=1,n+2 \\ F_{n+3,j}=\hat{F}_j(0) \quad j=1,n+2 \\ F_{n+4,j}=\hat{F}_j(1) \quad j=1,n+2 \\ \text{the other terms are null} \end{cases}$$

$[\mathbf{F0}]$: matrix ((n+4)x(n+4)),

$$\begin{cases} F0_{i,n+3} = F0(s_i) = -W^*(s_i,0)\theta_1 + \dfrac{W^*(s_i,1)}{(1+K1(1))}\theta_{n+2}, \\ \quad i = 1\,,\, n+2 \\ F0_{n+3,n+3} = \hat{F}0(0) = -\hat{W}^*(0,0) + \dfrac{\hat{W}^*(0,1)}{(1+K1(1))} \\ F0_{n+4,n+3} = \hat{F}0(1) = -\hat{W}^*(1,0) + \dfrac{\hat{W}^*(1,1)}{(1+K1(1))}, \\ \text{the other terms are null} \end{cases}$$

$\{P\}$: vector (1 x (n+4)),

$$\begin{cases} P_i = P(s_{i+1}) & i = 1\,,\, n+2 \\ P_{n+3} = \hat{P}(0) \\ P_{n+4} = \hat{P}(1) \end{cases}$$

ACKNOWLEDGMENTS

The authors wish to greatly thank the 'Ministère de l'Enseignement Supérieur et de la Recherche Scientifique' and the center 'CNRST' of Morocco and the center 'CNRS' of France for financial support from both projects: "PROTARS III (D11/22)" and "Action Intégrée (MA/05/17)".

REFERENCES

[1] Rosa M. A. Auciello N. M. Free vibrations of tapered beams with flexible ends. Journal of Computers and Structures 1996; 60 N°2: 197-202.
[2] Naguleswaran S. Comments on vibration of non-uniform rods and beams. Journal of Sound and Vibration 1996; 195: 197-202.
[3] Wu J. S., Hsieh M. Free vibration analysis of a non uniform beam with multiple point masses. Structural Engineering and Mechanics 2000; 9: 449-467.
[4] Chen D. W., Wu J-S. The exact solution for the natural frequencies and mode shapes of non uniform beam with multiple spring-mass systems. Journal of Sound and Vibration 2002; 255 (2): 299-232.
[5] El Felsoufi Z., Azrar L. Buckling, flutter and vibration analyses of beams by integral equation formulations. Computers and Structures 2005; 83: 2632-2649
[6] El Felsoufi Z., Azrar L. Integral equation formulation and analysis of the dynamic stability of damped beams subjected to sub-tangential follower forces. Journal of Sound and Vibration; 296 (2006) 690–713
[7] Nardini D., Brebbia CA. A new approach to free vibration analysis using boundary elements. In: Brebbia CA, editor. Boundary element method in engineering, Berlin: Springer, 1982: 313-26.
[8] Beskos D. E. Boundary element methods in dynamic analysis. Part II (1986-1996). Appl. Mech. Rev. ASME 1997; 50: 149-97.
[9] Karimi Khorramadi and A.R. Nezamabadi. Vibration Analysis of Functionally Graded Engesser- Timoshenko Beams Subjected to Axial Load Located on a Continuous Elastic Foundation, World Academy Science, Engineering and Technology, International Journal of Mechanical, Aerospace, Industrial and Mechatronics Engineering Vol:8, No:10, 2015.
[10] Timoshenko SV, Gere JM. *Theory of Elastic Stability*. New York: McGraw-Hill, 1961.
[11] El Felsoufi Z., Hachi H. Conception et Réalisation d'un dispositif de mesure de vibration de l'OCP, Maroc Phosphore I; PFE, EMI, Rabat, Maroc, 1994.